A hybrid explicit-implicit staggered-grid finite-difference scheme for the first-order acoustic wave-equation modeling

Yanfei Wang
Institute of Geology and Geophysics
Jingjie Cao
Hebei GEO University
Wenquan Liang (onethink2002@foxmail.com)
Longyan University

Research Article

Keywords:

Posted Date: January 17th, 2022

DOI: https://doi.org/10.21203/rs.3.rs-1254358/v1

Abstract

Implicit staggered-grid finite-difference (ISGFD) methods are widely used for the first-order acoustic wave-equation modeling. The identical ISGFD operator is commonly used for all of the first-order spatial derivatives in the first-order acoustic wave-equation. In this paper, we propose a hybrid explicit-implicit SGFD (HEI-SGFD) scheme which could simultaneously preserve the wave-equation simulation accuracy and increase the wave-equation simulation speed. We use a second-order explicit SGFD (ESGFD) operator for half of the first-order spatial derivatives in the first-order acoustic wave-equation. At the same time, we use the ISGFD operator with added points in the diagonal direction for the other first-order spatial derivatives in the first-order acoustic wave-equation. The proposed HEI-SGFD scheme nearly doubles the wave-equation simulation speed compared to the ISGFD schemes. In essence, the proposed HEI-SGFD scheme is equivalent to the second-order FD scheme with ordinary grid format. We then determine the HEI-SGFD coefficients in the time-space domain by minimizing the phase velocity error using the least-squares method. Finally, the effectiveness of the proposed method is demonstrated by a dispersion analysis and numerical simulations.

Introduction

Finite difference time domain methods are widely used in exploration seismology [1, 2, 3]. Staggered-grid finite-difference (SGFD) methods are part of the FDTD methods and are commonly utilized in seismic wave extrapolation because of their high accuracy, less memory requirement and easy implementation [4, 5, 6, 7].

To improve the accuracy and efficiency of the FD method, the FD stencil with added points in the diagonal direction was adopted[8, 9, 10]. Compared to the previous high-order FD stencils, the use of these new FD stencils could improve the wave-equation simulation efficiency while preserve the high accuracy by using a larger time step. Both of the ESGFD scheme and the ISGFD scheme are widely used for wave-equation modeling. The ISGFD scheme could achieve higher accuracy with much shorter FD operator compared with the ESGFD scheme [11, 12]. Another way to improve the accuracy and efficiency of the FDTD method is utilizing optimized FD operator coefficients [13, 14,15,16,17].

Normally, the identical SGFD operator is used for all of the first-order spatial derivatives in the first-order acoustic wave-equation. We proposed using different SGFD operators for different spatial derivatives in the acoustic wave equation[18, 19] and propose a HEI-SGFD scheme in this paper. We use the second-order ESGFD scheme for some of the first-order spatial derivatives in the first-order acoustic wave-equation. Meanwhile we use the high-order ISGFD scheme with added points in the diagonal direction for the rest of the first-order spatial derivatives. The proposed FD scheme is called the HEI-SGFD scheme. This HEI-SGFD scheme could save about 45 percent of the computational time compared with the ISGFD scheme while it still preserves high accuracy.

Theory

The first-order velocity-stress acoustic wave-equation can be described as follows:

$$\frac{\partial p}{\partial t} = -\rho v^2 \left(\frac{\partial V_z}{\partial z} + \frac{\partial V_x}{\partial x} \right), \tag{1}$$

$$\frac{\partial V_x}{\partial t} = -\frac{1}{\rho} \frac{\partial p}{\partial x}, \tag{2}$$

$$\frac{\partial V_z}{\partial t} = -\frac{1}{\rho} \frac{\partial p}{\partial z}. \tag{3}$$

where p is the pressure, ρ is the density and v is the wave propagation speed, V_x and V_z are the particle velocities. A constant density is assumed for the equations in this paper.

The acoustic wave-equation (1-3) can be discretized as

$$p_{i,j}^{k} = p_{i,j}^{k-1} - v^2\tau\left(\Delta_z V_{z_{(i+1/2,j)}}^{k+1/2} + \Delta_x V_{x_{(i,j+1/2)}}^{k+1/2}\right),$$

4

$$V_{x_{(i,j+1/2)}}^{k+1/2} = V_{x_{(i,j+1/2)}}^{k-1/2} - \tau\left(\Delta_x p_{i,j}^{k}\right),$$

5

$$V_{z_{(i+1/2,j)}}^{k+1/2} = V_{z_{(i+1/2,j)}}^{k-1/2} - \tau\left(\Delta_z p_{i,j}^{k}\right),$$

6

whereis the time step, $\varsigma_{m,j}^{n} = \varsigma(z + mh, x + jh, t + n\tau)$, $\varsigma = [V_z, V_x, p]$. The symbol Δ represents the implicit discrete form of the spatial derivative, for example

$$q_{i,j+1/2}^{k} = \Delta_x p_{i,j+1/2}^{k} = \frac{\frac{1}{h}\sum_{m=1}^{M} c_m(p_{i,j+m}^{k} - p_{i,j-m+1}^{k}) + \frac{1}{h}c_{M+1}(p_{i+1,j+1}^{k} - p_{i+1,j}^{k} + p_{i-1,j+1}^{k} - p_{i-1,j}^{k})}{1 + bh^2\frac{\delta^2}{\delta x^2}},$$

7

where

$$\frac{\delta^2 q}{\delta x^2} = \frac{q(x+h) + q(x-h) - 2q(x)}{h^2},$$

8

.

in which, M is the length of the SGFD operators, c_m and b are the SGFD coefficients and h is the grid size. M=7 and $c_{M+1} \neq 0$ are assumed in this paper in order to use a larger time and space grid interval.

Then we can implicitly get an approximation to the spatial derivative $q \approx \partial p/\partial x$as

$$bq_{i,j+3/2}^{k} + (1-2b)q_{i,j+1/2}^{k} + bq_{i,j-1/2}^{k} = \frac{1}{h}\left(\sum_{m=1}^{M} c_m(p_{i,j+m}^{k} - p_{i,j-m+1}^{k}) + c_{M+1}(p_{i+1,j+1}^{k} - p_{i+1,j}^{k} + p_{i-1,j+1}^{k} - p_{i-1,j}^{k})\right).$$

9

Hereafter, we denote Eqs. (4), (5) and (6) as the ISGFD scheme. One can use a larger time step with the coefficient c_{M+1}. At the same time, one can use a short operator length with the coefficient b[11, 12]. We propose to use the simplest explicit second-order SGFD operator for the spatial derivatives in Eqs. (2) and (3). This approach differs from the previous SGFD methods that use the same ISGFD operator for all of the first-order spatial derivatives in Eqs. (1), (2) and (3). The proposed HEI-SGFD scheme is given by:

$$p_{i,j}^{k} = p_{i,j}^{k-1} - v^2\tau\left(\Delta_z V_{z_{(i+1/2,j)}}^{k+1/2} + \Delta_x V_{x_{(i,j+1/2)}}^{k+1/2}\right),$$

10

$$V_{x_{(i,j+1/2)}}^{k+1/2} = V_{x_{(i,j+1/2)}}^{k-1/2} - \frac{\tau}{h}(p_{i,j+1}^{k} - p_{i,j}^{k}),$$

11

$$V_{z\,(i+1/2,j)}^{k+1/2} = V_{z\,(i+1/2,j)}^{k-1/2} - \frac{\tau}{h}(p_{i+1,j}^{k} - p_{i,j}^{k}).$$

12

The SGFD scheme in Eq. (10) is implicit while the SGFD scheme in Eqs. (11) and (12) are explicit; therefore, we refer the proposed SGFD scheme as the HEI-SGFD scheme. The HEI-SGFD scheme is an ISGFD scheme although some of spatial derivatives are approximated with explicit SGFD scheme. It seems that Eqs. (11) and (12) are not accurate. However, this is not the case. The SGFD coefficient in Eq. (10) is determined by considering Eqs. (11) and (12). It is easily observed that the proposed HEI-SGFD scheme in Eqs. (10)- (12) needs less floating-point computations compared with the ISGFD scheme given in Eqs. (4)-(6). The computational resources needed by Eqs. (11) and (12) are smaller than the computational resources needed by Eqs. (5) and (6).

Substitute Eqs. (11) and (12) into Eq. (10) and we get:

$$p_{i,j}^{k+1} = 2p_{i,j}^{k} - p_{i,j}^{k-1} - v^2\tau^2 \frac{\frac{1}{h^2}\sum_{m=1}^{M} c_m (p_{i+m,j}^{k} - p_{i-m-1,j}^{k} - p_{i-m+1,j}^{k} + p_{i-m,j}^{k}) + \frac{1}{h^2} c_{M+1}(p_{i+1,j+1}^{k} + p_{i-1,j+1}^{k} + p_{i+1,j-1}^{k} + p_{i-1,j-1}^{k})}{1 + bh^2\frac{\delta^2}{\delta x^2}}$$
$$- v^2\tau^2 \frac{\frac{1}{h^2}\sum_{m=1}^{M} c_m (p_{i,j+m}^{k} - p_{i,j+m-1}^{k} - p_{i,j-m+1}^{k} + p_{i,j-m}^{k}) + \frac{1}{h^2} c_{M+1}(p_{i+1,j+1}^{k} + p_{i-1,j+1}^{k} + p_{i+1,j-1}^{k} + p_{i-1,j-1}^{k})}{1 + bh^2\frac{\delta^2}{\delta x^2}}. \quad (13)$$

Eq. 13 can also be written as

$$p_{i,j}^{k+1} = 2p_{i,j}^{k} - p_{i,j}^{k-1} - \frac{v^2\tau^2}{h^2} \frac{-2c_1 p_{i,j}^{k} + \sum_{m=1}^{M-1}(c_m - c_{m+1})(p_{i+m,j}^{k} + p_{i-m,j}^{k}) + c_M(p_{i+M,j}^{k} + p_{i-M,j}^{k}) + c_{M+1}(p_{i+1,j+1}^{k} + p_{i-1,j+1}^{k} + p_{i+1,j-1}^{k} + p_{i-1,j-1}^{k})}{1 + bh^2\frac{\delta^2}{\delta x^2}}$$
$$- \frac{v^2\tau^2}{h^2} \frac{-2c_1 p_{i,j}^{k} + \sum_{m=1}^{M-1}(c_m - c_{m+1})(p_{i,j+m}^{k} + p_{i,j-m}^{k}) + c_M(p_{i,j+M}^{k} + p_{i,j-M}^{k}) + c_{M+1}(p_{i+1,j+1}^{k} + p_{i+1,j-1}^{k} + p_{i-1,j+1}^{k} + p_{i-1,j-1}^{k})}{1 + bh^2\frac{\delta^2}{\delta x^2}}. \quad (14)$$

In theory, the first-order HEI-SGFD scheme in Eqs. (10)- (12) is equivalent to the second-order implicit FD scheme with ordinary grid format as shown in Eq. (14).

The dispersion relation of the proposed HEI-SGFD scheme is

$$\left[-2\sin(0.5k_x h)\sum_{m=1}^{M} 2c_m \sin((m-0.5)k_x h) + 4c_{M+1}\cos(k_z h)(\cos(k_x h) - 1)\right]\left[1 + 2b(\cos(k_z h) - 1)\right]$$
$$+ \left[-2\sin(0.5k_z h)\sum_{m=1}^{M} 2c_m \sin((m-0.5)k_z h) + 4c_{M+1}\cos(k_x h)(\cos(k_z h) - 1)\right]\left[1 + 2b(\cos(k_x h) - 1)\right] \quad (15)$$
$$= \frac{1}{r^2}\left[1 + 2b(\cos(k_x h) - 1)\right]\left[1 + 2b(\cos(k_z h) - 1)\right]\left[2\cos(kv\tau) - 2\right]$$

The SGFD coefficient in Eq. (15) should be carefully determined with the optimization methods. Similar to the method proposed by Wang et al.[20], we get the objective function from Eq. 15 by minimizing the error between the true velocity and the phase velocity:

$$\Phi(c) = \sum_{k=3\text{e-}12}^{K}\sum_{\theta=0}^{\pi/4}\left(\frac{V_{fd}}{V} - 1\right)^2 = \sum_{k=3\text{e-}12}^{K}\sum_{\theta=0}^{\pi/4}\left(\frac{a\cos\left(1 + \frac{r^2 g}{2\left[1 + 2b\left(\cos\left(k_z h\right) - 1\right)\right]\left[1 + 2b\left(\cos\left(k_x h\right) - 1\right)\right]}\right)}{kv\tau} - 1\right)^2,$$

16

where

$$g= \left[-2\sin\left(0.5k_xh\right)\sum_{m=1}^{M}2c_m\sin\left((m-0.5)k_xh\right)+4c_{M+1}\cos(k_zh)(\cos(k_xh)-1)\right]\left[1+2b(\cos(k_zh)-1)\right]$$

$$+\left[-2\sin\left(0.5k_zh\right)\sum_{m=1}^{M}2c_m\sin\left((m-0.5)k_zh\right)+4c_{M+1}\cos(k_xh)(\cos(k_zh)-1)\right]\left[1+2b(\cos(k_xh)-1)\right].$$

17

The only unknowns in Eq. (16) are $c_m\,(m=1,\cdots,M+1)$ and b. The wave number k in Eq. (16) should start from zero. However, there is k in the denominator, which causes instability. Therefore, we let k start from a very small number, e.g., 3e-12. We assume that the parameters such as the wave propagation speed, the time step and the spatial grid intervals are already given (then $r = v\tau/h$ will be known). The other two parameters are k and θ. The propagation angle θ is from 0 to $\pi/4$ (0, $\pi/16$, $2\pi/16$ ... $\pi/4$). From Eq. (16), we found that in the frequency-wave number domain the SGFD coefficients are related to the Courant ratio r. When one considers a wave-equation simulation with both fixed time and spatial steps grid intervals, the SGFD coefficient is different for different velocities and the stencil forms a big 3D matrix for a 2D complex velocity model. In order to get the hybrid explicit-implicit SGFD coefficient we apply the MATLAB function *lsqnonlin* to solve the nonlinear least-squares problem in Eq. (16).

The proposed HEI-SGFD scheme can be easily extended to 3D:

$$p_{l,m,n}^{k}=p_{l,m,n}^{k-1}-v^2\tau\left(\Delta_z V_{z}^{\,k-1/2}{}_{(l,m,n)}+\Delta_x V_{x}^{\,k-1/2}{}_{(l,m,n)}+\Delta_y V_{y}^{\,k-1/2}{}_{(l,m,n)}\right),$$

18

$$V_{x}^{\,k+1/2}{}_{(l,m+1/2,n)}=V_{x}^{\,k-1/2}{}_{(l,m+1/2,n)}-\frac{\tau}{h}(p_{l,m+1,n}^{k}-p_{l,m,n}^{k}),$$

19

{V_y}_{{(l,m.n+1/2)}}^{{k+1/2}}={V_y}_{{(l,m.n+1/2)}}^{{k-1/2}}-\frac{\tau }{h}(p_{{l,m,n+1}}^{k}-p_{{l,m,n}}^{k}),

20

{V_z}_{{(l+1/2,m,n)}}^{{k+1/2}}={V_z}_{{(l+1/2,m,n)}}^{{k-1/2}}-\frac{\tau }{h}(p_{{l+1,m,n}}^{k}-p_{{l+1,m,n}}^{k}).

21

whereis the time step, \varsigma _{{l,m,n}}^{k}=\varsigma (z+lh,x+mh,y+nh,t+k\tau),\varsigma =[{V_z},{V_x},{V_y},p].The SGFD coefficient in Eq. (18) of the hybrid explicit-implicit SGFD scheme for 3D can be determined similarly.

Dispersion Analysis And Stability Analysis

In the following, we will demonstrate that the proposed HEI-SGFD scheme possesses similar accuracy compared to the computational-intensive traditional implicit SGFD scheme.

The 2D dispersion error of the HEI-SGFD scheme is defined as follows

\delta =\frac{{{v_{FD}}}}{v}=\frac{1}{{krh}}a\cos \left({1+\frac{{{r^2}}}{2}\frac{g}{{\left[{1+2b(\cos ({k_x}h)-1)} \right]\left[{1+2b(\cos ({k_z}h)-1)} \right]}}} \right)

22

The difference between the FD propagation time and the exact propagation time through one grid is defined as

$$\varepsilon = \frac{h}{v_{FD}} - \frac{h}{v} = \frac{h}{v}\left(\frac{v}{v_{FD}} - 1\right) = \frac{h}{v}\left(\frac{1}{\delta} - 1\right) \qquad (23)$$

Figure 1 shows the dispersion error curves for the traditional ISGFD scheme and the HEI-SGFD scheme with the SGFD coefficient optimized in the time-space domain for different velocities. The spatial grid interval is 20m and the time step is 2.5ms. The velocities are 1500 m/s for Figure 1 (a) and (c), and 4500 m/s for Figure 1 (b) and (d), respectively. The ISGFD coefficients used in Figure 1 (a) and (b) are shown in Table 1. The HEI-SGFD coefficients used in Figure 1 (c) and (d) are shown in Table 2. We observed that the ISGFD method can preserve the dispersion relation at a large frequency range even when *M* (which characterizes the width of the stencil is equal to 3. The grid dispersion in Figure 1(c) and (d) is similar to the one in Figure 1 (a) and (b). However, the wave-equation simulation speed could be nearly doubled with the HEI-SGFD scheme.

Table 1
The ISGFD coefficients used to obtain the dispersion error curves in Fig. 1. The first and second rows are the ISGFD coefficients used for Fig. 1(a) and (b). The third and fourth rows are the HEI-SGFD coefficients used for Fig. 1(c) and (d).

v	c_1	c_2	c_3	c_4	*b*	*r*
1500	0.491536	0.176179	-0.00451725	0.00111733	0.195121	0.1875
4500	0.499944	0.162557	-0.00178656	0.0106658	0.180653	0.5625
1500	0.55651	0.159946	-0.00839528	0.00251221	0.201776	0.1875
4500	0.506957	0.156756	-0.00429556	0.0220486	0.191268	0.5625

When applying the Fourier transforms to the SGFD operators for the spatial derivatives in Eq. 7, we get

{k_x} \approx \frac{{ - \left({\sum\limits_{{m=1}}^{M} {2{c_m}} \sin \left({(m - 0.5){k_x}h} \right)+{\text{4}}{c_{M+1}}\sin ({k_x}h/2)\cos ({k_z}h)} \right)}}{h\left({{\text{1+2}}b{\text{(cos()}{k_x}h{\text{())}} - {\text{1)}}} \right)}}.
24

Similarly, we can get

{k_z} \approx \frac{{ - \left({\sum\limits_{{m=1}}^{M} {2{c_m}} \sin \left({(m - 0.5){k_z}h} \right)+{\text{4}}{c_{M+1}}\sin ({k_z}h/2)\cos ({k_x}h)} \right)}}{h\left({{\text{1+2}}b{\text{(cos()}{k_z}h{\text{())}} - {\text{1)}}} \right)}}
25

Then we can get the dispersion relation for the ISGFD scheme

\begin{gathered} - {\left[{\sum\limits_{{m=1}}^{M} {2{c_m}} \sin \left({(m - 0.5){k_x}h} \right)+{\text{4}}{c_{M+1}}\sin ({k_x}h/2)\cos ({k_z}h)} \right]^2}{\left[{{\text{1+2}}b{\text{(cos()}{k_z}h{\text{())}} - {\text{1)}}} \right]^{\text{2}}} \hfill \\ - {\left[{\sum\limits_{{m=1}}^{M} {2{c_m}} \sin \left({(m - 0.5){k_z}h} \right)+{\text{4}}{c_{M+1}}\sin ({k_z}h/2)\cos ({k_x}h)} \right]^2}{\left[{{\text{1+2}}b{\text{(cos()}{k_x}h{\text{())}} - {\text{1)}}} \right]^{\text{2}}} \hfill \\ =\frac{1}{{{r^2}}}{\left[{{\text{1+2}}b{\text{(cos()}{k_x}h{\text{())}} - {\text{1)}}} \right]^{\text{2}}}{\left[{{\text{1+2}}b{\text{(cos()}{k_z}h{\text{())}} - {\text{1)}}} \right]^{\text{2}}}\left[{2\cos \left({kv\tau } \right) - 2} \right] \hfill \\ \end{gathered}
26

From Eq. (28) we get the CFL condition for the ISGFD scheme:

r \leqslant s=\sqrt {\frac{{2{\left[{{\text{1}} - {\text{4}}b} \right]}^{\text{2}}}}{{{\left[{\sum\limits_{{m=1}}^{M} {2{c_m}} {{(- 1)}^{m - 1}} - {\text{4}}{c_{M+1}}} \right]}^2}}}
27

From dispersion relation Eq. (16), we can get:

{\text{ }}\frac{{{r^2}g}}{{\left[{{\text{1+2}}b{\text{(cos()}}{k_x}h{\text{()}} - {\text{1)}}} \right]\left[{{\text{1+2}}b{\text{(cos()}}{k_z}h{\text{()}} - {\text{1)}}} \right]}} \geqslant - 4
28

Then the stability condition of the HEI-SGFD scheme can be obtained as follows

r \leqslant s=\sqrt {\frac{{{\text{1-4}}b}}{{\sum\limits_{{m=1}}^{M} {2{c_m}} {{(- 1)}^{m - 1}} - 4{c_{M+1}}}}}
29

Figure 2 illustrates the stability condition of the ISGFD scheme and the HEI-SGFD scheme. The stability condition of the ISGFD scheme is that r is less than 0.715. The stability condition of the HEI-SGFD scheme is that r is less than 0.75. This means that the HEI-SGFD scheme has a better stability condition than the ISGFD scheme. We use the wave-equation simulation to verify the soundness of the stability condition. At first, we set h=10m, v=740m/s and \tau =1ms (so that r = 0.74). It yields that for the ISGFD scheme, it is unstable. Nevertheless, the HEI-SGFD scheme is stable. This further indicates that the HEI-SGFD scheme has a better stability condition than the traditional ISGFD scheme.

Examples

We first consider a homogeneous model. The seismic source position is at the surface of the model. The wave propagation speed is 2800m/s and the spatial grid interval is 10m. The time step is 2ms for the FD methods. A Ricker wavelet with a main frequency at 20.7Hz is used as seismic source.

The snapshots of the p obtained by 3 different wave extrapolation methods are presented in Fig. 3. Both of the ISGFD coefficients in Fig. 3(a) and (b) are determined in the time-space domain by the least-squares method. Table 2 shows the FD coefficients for the ISGFD scheme and the HEI-SGFD scheme. Table 3 shows the implicit second-order normal-grid FD coefficients obtained from the HEI-SGFD scheme (Fig. 3d). We note that Table 3 could be directly obtained from the last row of Table 2 by [-2c_1 c_1-c_2 c_2-c_3 c_3 c_4 b] according to Eq. 14.

From Fig. 3(a)-(c), we can observe that the snapshots obtained by the ISGFD scheme and the HEI-SGFD scheme are almost identical to each other. However, the cost of computation of the HEI-SGFD scheme is about 55 percent of the ISGFD scheme. In our simulation, there are 499 grid points in the z direction and 499 grid points in the x direction. With the ISGFD scheme, the simulation time is 44 seconds. With the proposed HEI-SGFD grid scheme, the simulation time is 24 seconds. The snapshots of the Vz and Vx components show similar pattern and we provide the source codes to the interested readers.

Table 2
The ISGFD coefficients used to obtain the snapshots in Fig. 3. The first row is the ISGFD coefficients used for Eqs. (4-6). The second row is the HEI-SGFD coefficients used for Eq. (10).

c_1	c_2	c_3	c_4	b	r
0.499559	0.162801	-0.00181516	0.0105621	0.180896	0.56
0.505632	0.15755	-0.004451	0.0218698	0.191784	0.56

Table 3
The implicit normal-grid FD coefficient obtained from the last row of Table 2 used to obtain the snapshot in Fig. 3d.

c_0	c_1	c_2	c_3	c_4	b	r
-1.01126	0.348082	0.162001	-0.004451	0.0218698	0.191784	0.56

Figure 4 shows the commonly used BP salt velocity model in geophysical community. There are 475 grid points in the z direction and 799 grid points in the x direction (this does not include the grid nodes for the absorbing boundary). The seismic source position is shown as a red star. The spatial sampling interval is 15m. The temporal step is 2ms for all of the FD methods. A Ricker wavelet with a dominant frequency at 14.3Hz was used as the seismic source.

Figure 5 shows the seismic records and seismograms for the *p* component obtained by the ISGFD scheme, the proposed HEI-SGFD scheme and the implicit FD scheme with ordinary grid format, respectively. From Figure 5(a)-5(d), it is observed that the seismic records are similar to each other for all the three methods. From Figure 5(e)-5(f), it can be further observed that the seismograms are overlapped to each other for all the three methods. However, with the proposed HEI-SGFD scheme, the simulation time is reduced by almost 45 percent. For example, in our simulation, with the ISGFD scheme, the simulation time is 325 seconds; while with the proposed HEI-SGFD grid scheme, the simulation time is 179 seconds. The significant reduction in simulation time is mainly resulted from that we use the simplest explicit SGFD operator in Eqs. (11) and (12).

Conclusion

We propose a HEI-SGFD scheme for the first-order acoustic wave-equation modeling in this paper. The proposed HEI-SGFD scheme possesses two major advantages compared to the ISGFD schemes. The first one is that the length of the SGFD operator in Eqs. (11) and (12) is much shorter than that of the SGFD operator in Eqs. (5) and (6). The second advantage is that, the SGFD operator in Eqs. (11) and (12) are explicit. Through dispersion analysis and numerical simulation, we conclude that the proposed HEI-SGFD scheme is more efficient than the ISGFD scheme while simultaneously preserving high accuracy. For reproducibility, we provide the source code. As a result, the HEI-SGFD scheme could be widely adopted for first-order acoustic wave-equation simulations.

Declarations

Acknowledgements

We thank Ursula Iturraran-Viveros of Universidad Nacional Autónoma de México for helpful discussions. This research is supported by the National Natural Science Foundation of China under grant numbers 41704120 and 41674114, the Education Department of Fujian Province under grant number 2018[47], IGGCAS grant 2019031 and CAS innovation program ZDBS-LY-DQC003 are also acknowledged.

References

1. Kelly K R, Ward R W, Treitel S, et al. Synthetic seismograms: A finite-difference approach. *Geophysics*, 41(1): 2–27. https://doi.org/10.1190/1.1440605 (1976)
2. Alford R M, Kelly K R, Boore D M. Accuracy of finite-difference modeling of the acoustic wave equation. *Geophysics* 39(6): 834–842. https://doi.org/10.1190/1.1440470 (1974)
3. Igel H, Mora P, Riollet B. Anisotropic wave propagation through finite-difference grids. *Geophysics* 60(4): 1203–1216. https://doi.org/10.1190/1.1443849 (1995)
4. Virieux, J. SH-wave propagation in heterogeneous media: Velocity-stress finite-difference method. *Geophysics* 49(11), 1933-1942. https://doi.org/10.1190/1.1441605 (1984).
5. Virieux, J. P-SV wave propagation in heterogeneous media: Velocity-stress finite-difference method. *Geophysics* 51(4), 889–901. https://doi.org/10.1190/1.1442147 (1986).
6. Yao, G., Wu, D. & Debens, H. Adaptive finite difference for seismic wavefield modelling in acoustic media. *Sci Rep* 6, 30302. https://doi.org/10.1038/srep30302 (2016).
7. Schaeken, T., Hoogerbrugge, L. & Verschuur, E. A non-reflecting wave equation through directional wave-field suppression and its finite difference implementation. *Sci Rep* 12, 407. https://doi.org/10.1038/s41598-021-04064-3 (2022).
8. Tan, S., & Huang, L. An efficient finite-difference method with high-order accuracy in both time and space domains for modeling scalar-wave propagation. Geophysical Journal International, 197(2), 1250–1267. https://doi.org/10.1093/gji/ggu077(2014).
9. Liu, H., Dai, N., Niu, F., Wu, W. An explicit time evolution method for acoustic wave propagation. Geophysics, 79(3) T117-T124. https://doi.org/10.1190/geo2013-0073.1 (2014).
10. Xu S, Bao Q, Ren Z, et al. Applying an advanced temporal and spatial high-order finite-difference stencil to 3D seismic wave modeling. *Journal of Computational Physics* 436: 110133. (2021)
11. Claerbout, J. F. Imaging the Earth's Interior (Blackwell Scientific Publications Ltd, GBR, 1985).
12. Liu, Y., & Sen, M. K. A practical implicit finite-difference method: examples from seismic modelling. *Journal of Geophysics and Engineering* 6(3), 231–249. https://doi.org/10.1088/1742-2132/6/3/003 (2009).
13. Chu, C. & Stoffa, P. Determination of finite-difference weights using scaled binomial windows. *Geophysics* 77, W17–W26. https://doi.org/10.1190/geo2011-0336.1 (2012).

14. Zhang, J. & Yao, Z. Optimized finite-difference operator for broadband seismic wave modeling. *Geophysics* 78, A13–A18. https://doi.org/10.1190/geo2012-0277.1 (2012).
15. Zhang, J. & Yao, Z. Optimized explicit finite-difference schemes for spatial derivatives using maximum norm. *J. Comput. Phys. 2*50, 511–526. https://doi.org/10.1016/j.jcp.2013.04.029 (2013).
16. Liang, W., Wang, Y. & Yang, C. Determining finite difference weights for the acoustic wave equation by a new dispersion-relationship-preserving method. *Geophys. Prospect.* 63, 11–22 https://doi.org/10.1111/1365-2478.12160 (2015).
17. Yang D, Tong P, Deng X. A central difference method with low numerical dispersion for solving the scalar wave equation. *Geophys. Prospect*, 60(5):885–905. https://doi.org/10.1111/j.1365-2478.2011.01033.x (2012)
18. Liang W, Wu X, Wang Y, et al. A new staggered grid finite difference scheme optimized in the space domain for the first order acoustic wave equation. *Exploration Geophysics* 49(6):898–905. https://doi.org/10.1071/EG17088 (2018).
19. Liang W, Wu X, Wang Y, et al. A simplified staggered-grid finite-difference scheme and its linear solution for the first-order acoustic wave-equation modeling. *Journal of Computational Physics* 374: 863–872. https://doi.org/10.1016/j.jcp.2018.08.011 (2018).
20. Wang, Y., Liang, W., Nashed, Z., Li, X., Liang, G., Yang, C. Seismic modeling by optimizing regularized staggered-grid finite-difference operators using a time-space-domain dispersion-relationship-preserving method. *Geophysics* 79(5), T277-T285. https://doi.org/10.1190/geo2014-0078.1 (2014).

Figures

Figure 1

Dispersion error curves for the different implicit SGFD schemes. The time step is 2.5ms and the spatial grid interval is 20m. (a) the ISGFD scheme with v=1500m/s; (b)the ISGFD scheme with v=4500m/s; (c)the HEI-SGFD scheme with v=4500m/s; (d) the HEI-SGFD scheme with v=4500m/s.

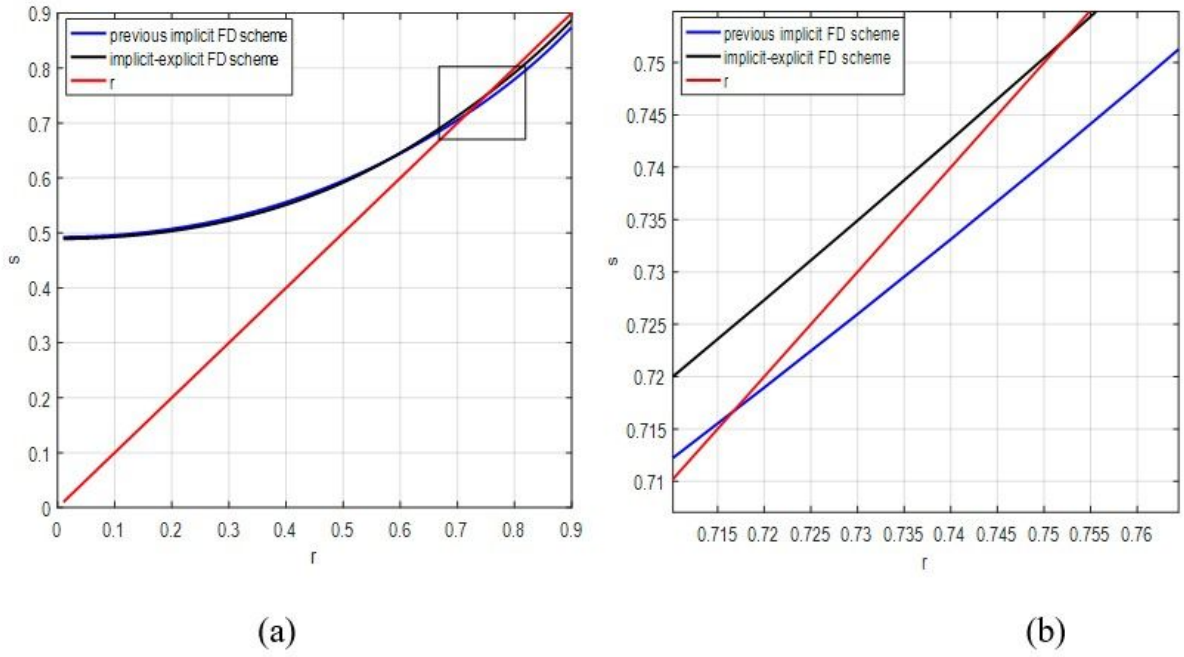

Figure 2

Comparison of the stability condition. (a) Stability condition of different implicit SGFD schemes; (b) local enlargement of Figure 2(a) in the rectangle.

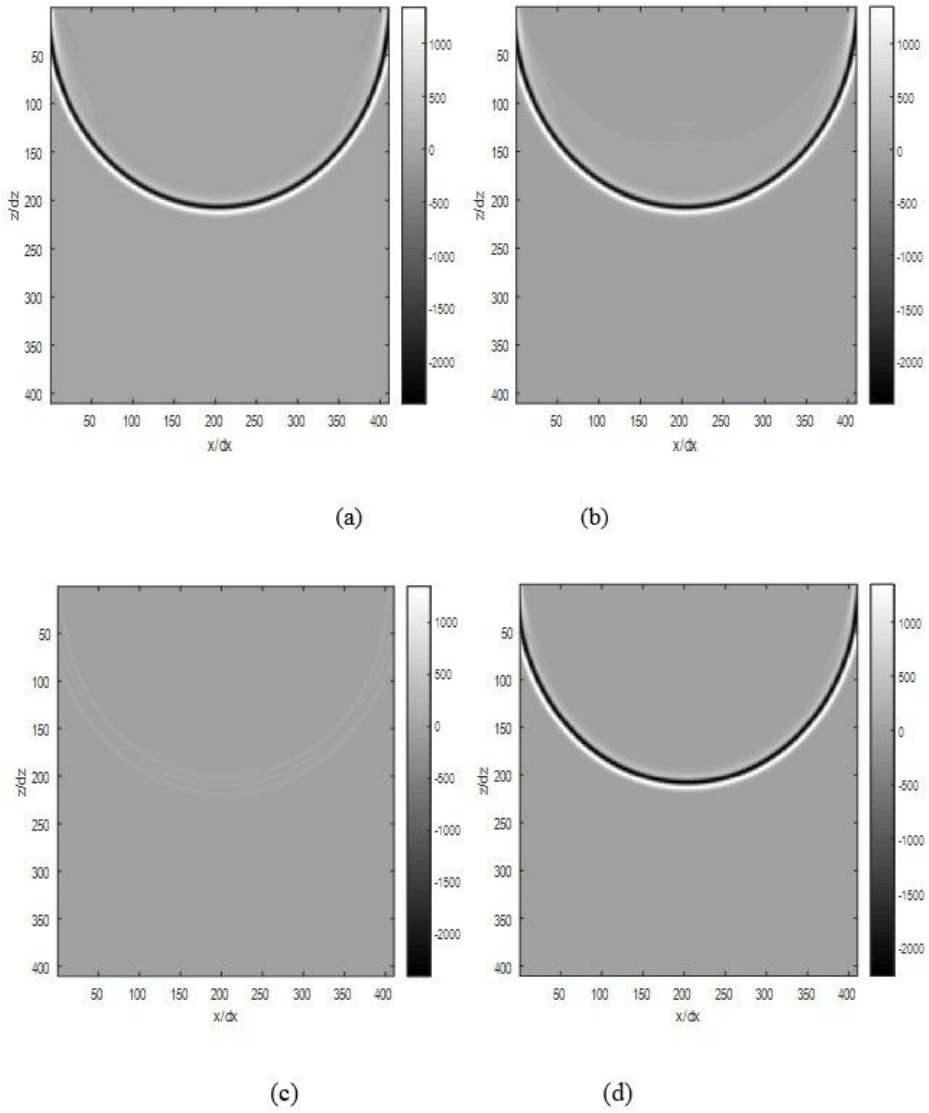

Figure 3

Snapshots *p* obtained with different SGFD schemes. (a) The lSGFD scheme; (b) the HEI-SGFD scheme; (c) the difference between Fig.3 (a) and 3(b); (d) the implicit FD scheme for second-order wave-equation obtained from the HEI-SGFD scheme.

Figure 4

The BP salt velocity model

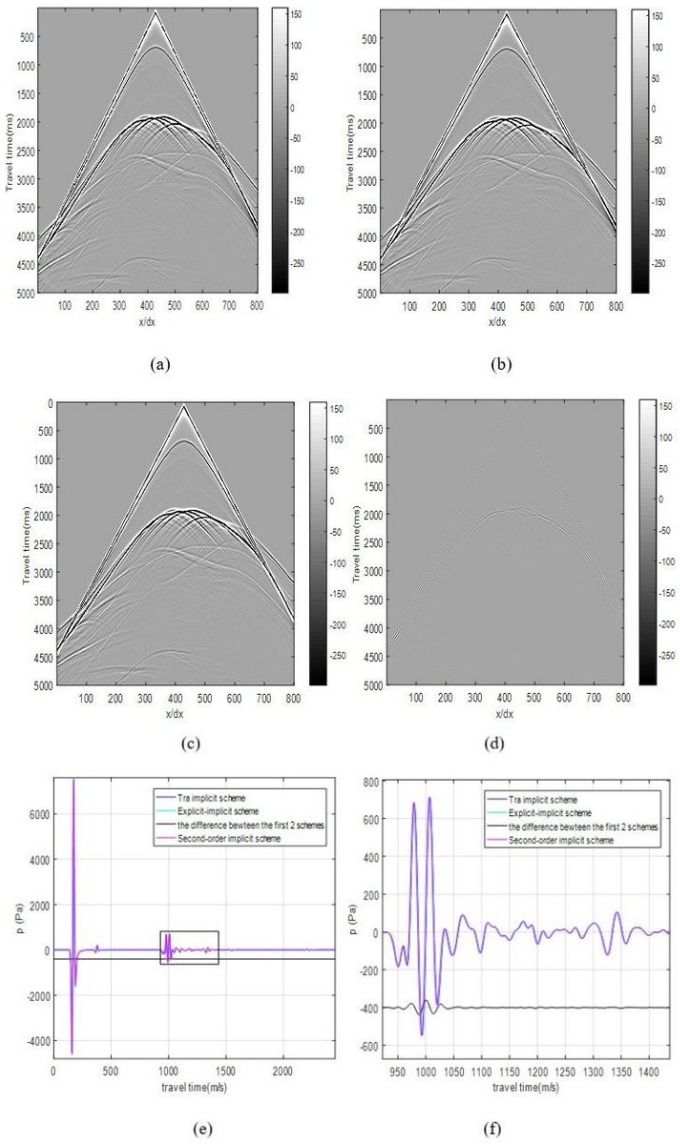

Figure 5

Seismic records *p* obtained with different FD schemes. (a) The ISGFD scheme; (b) the HEI-SGFD scheme; (c) the implicit FD scheme for second -order wave-equation obtained from the HEI-SGFD scheme; (d) the difference between Fig. 5(a) and 5(b); (e) the seismograms from Fig. 5(a)-5(c) at x/dx=405; (f) local enlargement of Fig. 5(e).

Supplementary Files

This is a list of supplementary files associated with this preprint. Click to download.

- Supplementarymaterial.txt